



An antiviral role for the RNA interference machinery in *Caenorhabditis elegans*

Citation

Schott, D. H., D. K. Cureton, S. P. Whelan, and C. P. Hunter. 2005. "An Antiviral Role for the RNA Interference Machinery in *Caenorhabditis Elegans*." *Proceedings of the National Academy of Sciences* 102 (51): 18420–24. <https://doi.org/10.1073/pnas.0507123102>.

Published version

<https://doi.org/10.1073/pnas.0507123102>

Link

<http://nrs.harvard.edu/urn-3:HUL.InstRepos:41483565>

Terms of use

This article was downloaded from Harvard University's DASH repository, and is made available under the terms and conditions applicable to Other Posted Material (LAA), as set forth at

<https://harvardwiki.atlassian.net/wiki/external/NGY5NDE4ZjgzNTc5NDQzMGIzZWZhMGFIOWI2M2EwYTg>

Accessibility

<https://accessibility.huit.harvard.edu/digital-accessibility-policy>

Share Your Story

The Harvard community has made this article openly available.

Please share how this access benefits you. [Submit a story](#)

An antiviral role for the RNA interference machinery in *Caenorhabditis elegans*

Daniel H. Schott*, David K. Cureton†, Sean P. Whelan†, and Craig P. Hunter**

*Department of Molecular and Cellular Biology, Harvard University, Cambridge, MA 02138; and †Department of Microbiology and Molecular Genetics, Harvard Medical School, Boston, MA 02115

Edited by Phillip A. Sharp, Massachusetts Institute of Technology, Cambridge, MA, and approved November 4, 2005 (received for review August 16, 2005)

RNA interference (RNAi) is a sequence-specific gene-silencing mechanism triggered by exogenous dsRNA. In plants an RNAi-like mechanism defends against viruses, but the hypothesis that animals possess a similar natural antiviral mechanism related to RNAi remains relatively untested. To test whether genes needed for RNAi defend animal cells against virus infection, we infected wild-type and RNAi-defective cells of the nematode *C. elegans* with vesicular stomatitis virus engineered to encode a GFP fusion protein. We show that upon infection, cells lacking components of the RNAi apparatus produce more GFP and infective particles than wild-type cells. Furthermore, we show that mutant cells with enhanced RNAi produce less GFP. Our observation that multiple genes required for RNAi are also required for resistance to vesicular stomatitis virus suggests that the RNAi machinery functions in resistance to viruses in nature.

vesicular stomatitis virus | virus

Gene silencing by RNA interference (RNAi) occurs largely through sequence-specific destruction of target messenger RNA (reviewed in refs. 1 and 2). Enzymes of the Dicer class cut dsRNA into short fragments known as small interfering RNAs, which direct cleavage of cognate ssRNA. Proteins of the Argonaute family required for RNAi might be responsible for this RNA cleavage (3). Both Dicer and Argonaute are conserved in a wide range of organisms that have RNAi, including plants, mammals, and *C. elegans*. Screens in *C. elegans* have identified many additional components involved in RNAi (4, 5), making *C. elegans* the organism with the greatest number of known parts of the RNAi apparatus.

Many viruses produce some dsRNA as a byproduct of their replication (reviewed in ref. 6), and dsRNA has long been known to be a potent trigger of nonspecific antiviral responses in mammalian cells involving the dsRNA-dependent protein kinase PKR and the 2',5'-oligoadenylate synthetase/RNase L system (reviewed in refs. 6 and 7). Because only traces of dsRNA are needed to trigger RNAi (8), it is widely assumed that one function of RNAi in animals is antiviral defense, and indeed, some animal viruses encode dsRNA-sequestering proteins, analogous to the RNAi inhibitors that are encoded by many plant viruses as an apparent countermeasure to host RNAi (reviewed in refs. 7 and 9–11). However, it is as yet unclear whether the animal virus dsRNA-sequestering proteins are a countermeasure against host RNAi or merely a countermeasure against the nonspecific dsRNA-triggered antiviral responses (reviewed in ref. 6).

The idea that components involved in RNAi provide a natural antiviral defense mechanism in animals has been tested in mosquito, but only for a single Argonaute-like gene (12). To test the role of multiple RNAi factors, we have developed an assay for viral infection of wild-type and mutant *C. elegans* cells. Because no natural virus of *C. elegans* is known, we infected worm primary embryonic cells (13) with vesicular stomatitis virus (VSV) (Indiana strain), a rhabdovirus whose natural hosts are biting flies and mammalian livestock. We find that VSV productively infects wild-type cells, that cells mutant for a variety

of RNAi components support greater virus production, that genetic enhancers of RNAi suppress viral gene expression, and that the source of the antiviral dsRNA trigger is autonomous to the infected cells.

Materials and Methods

Recombinant VSV Encoding Enhanced GFP–Phosphoprotein Fusion (rVSV::eGFP–P). We constructed the plasmid encoding the rVSV::eGFP–P genome in several steps:

(i) DNA fragments corresponding to the open reading of eGFP and nucleotides 121–1395 and 1399–3841 of the VSV genome were amplified by PCR from pGFP-N1 (Clontech) and the full-length cDNA clone of VSV [pVSV1(+)] (14), respectively. We fused the three fragments together by PCR and ligated the product into pGEM-T by using the pGEM-T Easy Vector System (Promega). eGFP primers were as follows: 5'-gaaaaaactaacagatatcatggtgagcaaggcg-3' and 5'-ctttgtgagattatcctgtacagctcgtccatg-3'. VSV 121–1395 primers were as follows: 5'-gcaaatgaggatccagtgg-3' and 5'-cgcccttgcaccatgatctgttagtctttttc-3'. VSV 1399–3841 primers were as follows: 5'-catggacgagctgtacaaggataatctcacaagaag-3' and 5'-atctcgaccagacacctg-3'.

(ii) We digested the resulting plasmid and pSWINT2 (a plasmid encoding nucleotides 1–3866 of the full-length VSV genome) with BstZ17I and XbaI, followed by ligation of the fragment containing the eGFP–P gene into pSWINT2 (pSWINT2–eGFP).

(iii) pVSV1(+) was digested with AvrII, SphI, and BglII, and the 7,702-bp fragment [corresponding to base pairs 3,717–11,418 of pVSV1(+)] was ligated into the AvrII and SphI sites of pSWINT2–eGFP–P.

(iv) We recovered rVSV::eGFP–P from plasmid DNA and prepared working stocks essentially as described (14). Because we found that the ability of virus stocks to infect *C. elegans* cells deteriorates much faster than their ability to infect mammalian cells at 4°C, we divided fresh virus stocks into small aliquots and stored them at –70°C.

Plaque Assays. We exposed confluent Vero African green monkey kidney cells in 3-cm wells to dilutions of virus in 200 μ l of medium for 1 h at 37°C with repeated shaking and overlaid the cells with 3 ml of medium containing 0.25% low gelling temperature agarose. After 30–40 h, incubation at 34°C, we fixed the cells in 10% formaldehyde for 1 h, removed the block of medium, and stained with 0.05% crystal violet in 10% ethanol. Medium from uninfected worm cells produced no plaques. Note that multiplicities of infection based on numbers of green fluorescent foci and spots in both wild-type and *rde-1(ne219)*

Conflict of interest statement: No conflicts declared.

This paper was submitted directly (Track II) to the PNAS office.

Abbreviations: RNAi, RNA interference; VSV, vesicular stomatitis virus; moi, multiplicity of infection; eGFP, enhanced GFP; P, phosphoprotein.

*To whom correspondence should be addressed. E-mail: hunter@mcb.harvard.edu.

© 2005 by The National Academy of Sciences of the USA

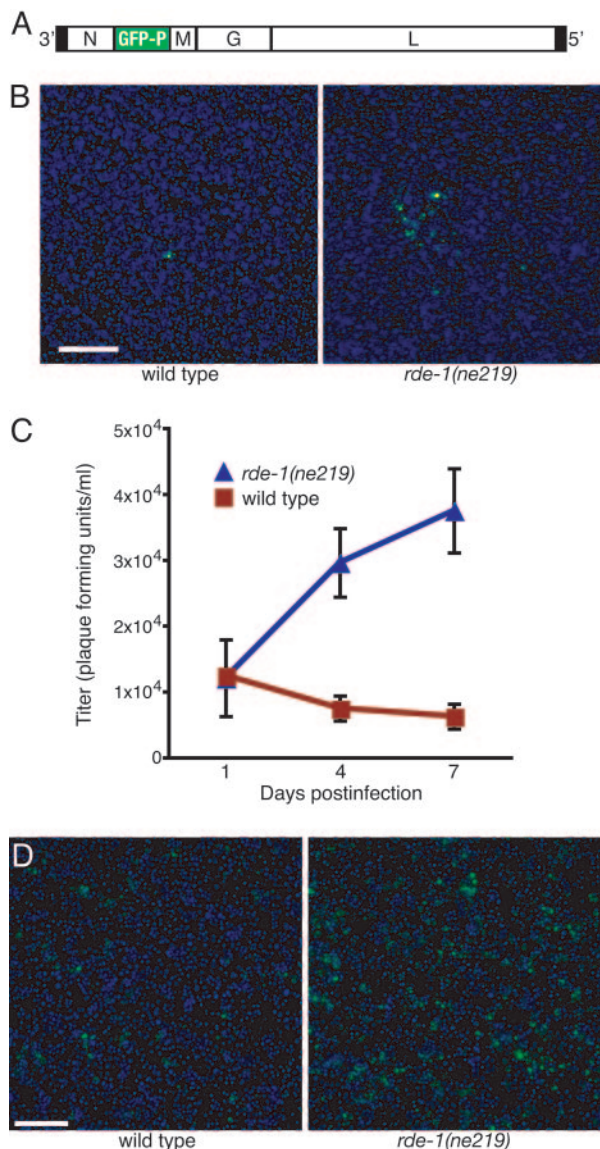


Fig. 1. VSV infection of wild-type and *rde-1* mutant *C. elegans* cells. (A) Schematic of the genome structure of the recombinant VSV used in this study, encoding a GFP-P fusion protein. (B) *C. elegans* cells 7 days after infection at moi = 0.003 (15). Green/yellow, GFP fluorescence; blue, Hoechst 33342 staining for DNA. (Scale bar, 100 μ m.) (C) Time course of virus titers capable of infecting mammalian cells, in medium after infection of wild type and *rde-1(ne219)* cells at moi = 3. Error bars represent SEM; $n = 3$ cell-culture wells. Titer in medium over *rde-1(ne219)* cells at day 7 is different from titer over wild-type cells at day 7 ($P = 0.03$ in two-tailed t test). (D) *C. elegans* cells 7 days after infection at moi = 3. Green, GFP fluorescence; blue, Hoechst 33342 staining for DNA. (Scale bar, 50 μ m.)

Genes Needed for Cell-Autonomous RNAi Inhibit VSV Infection. The first mutant we tested for effects on VSV infection is *rde-1(ne219)*. *rde-1* is one of 26 Argonaute-like genes in *C. elegans* and is required cell-autonomously for RNAi (4). Infection of *rde-1(ne219)* mutant cells at an moi of 0.003 results in larger clusters of green fluorescent cells than does infection of wild-type cells (Fig. 1B), suggesting that wild-type *rde-1* inhibits the spread of infection among cells and that at least one cycle of replication, budding, and reinfection occurs in the absence of *rde-1*. A corresponding increase in titers of infectious virus released into the cell culture medium is observed for the *rde-1(ne219)* mutant cells (Fig. 1C) infected at an moi of 3. By

Table 1. GFP levels in worm cells 7 days after infection at an moi of 3 after treatment with cycloheximide or mock treatment 24 h after infection

Strain	Treatment	
	Mock	1 μ g/ml cycloheximide
Wild type	(1*)	0.40
<i>rde-1(ne219)</i>	3.22	0.46

*Values are ratios of GFP fluorescence to Hoechst 33342 fluorescence, relative to mock-treated wild type. Cell morphology and numbers of nuclei appear to be unaffected by cycloheximide treatment.

contrast, wild-type cells produce little virus capable of reinfecting mammalian cells. At an moi of 3, *rde-1(ne219)* mutant cells produce approximately four times as much GFP as do wild-type cells (Figs. 1D and 2A).

We tested four additional *C. elegans* mutants defective for RNAi: *rde-3(ne298)*, *rde-4(ne301)*, *rrf-1(pk1417)*, and *sid-1(qt9)*. The first three of these genes are, like *rde-1*, required cell-autonomously for RNAi (4, 16). *rde-3* encodes a member of the polymerase beta nucleotidyltransferase superfamily (17), and *rde-4* encodes a dsRNA-binding protein that forms a complex with Dicer and RDE-1 (18), whereas *rrf-1* encodes a predicted RNA-directed RNA polymerase implicated in RNAi trigger RNA amplification (16). We found that *rde-3*, *rde-4*, and *rrf-1* are, like *rde-1*, required for resistance to VSV, as indicated by significantly higher GFP levels in the mutants compared with wild type (Fig. 2A). *sid-1*, which encodes a probable dsRNA channel and is required for the cell-to-cell spread of the RNAi signal in intact worms (19, 20) and for the initiation of RNAi in response to exogenous dsRNA in cultured cells (Christina Molodowitch and C.P.H., unpublished data), is dispensable for cell-autonomous RNAi. Importantly, the *sid-1(qt9)* mutant shows relatively little effect on GFP levels (Fig. 2A), indicating that the wild-type cells are not merely responding to traces of free dsRNA contaminating the VSV stock.

As well as measuring GFP production, we determined levels of VSV (–) strand in infected cells and VSV titers in the culture medium. *rde-1(ne219)*, *rde-3(ne298)*, *rde-4(ne301)*, and *rrf-1(pk1417)* cells accumulate more VSV (–) strand RNA than do wild-type cells (Fig. 2B). The increased amount of VSV (–) strand RNA in RNAi-defective mutants is consistent with an increase in viral genome replication in these cells. The numbers in Fig. 2B are probably a substantial underestimate of genome replication, because we suspect that only a small proportion of the virus used for infection enters the worm cells, survives, or leads to productive infection; the apparent titer of the virus stock for infection of worm cells is $\approx 1/50$ th of that for infection of mammalian cells (see note on plaque assays in *Materials and Methods*). Measurement of VSV (–) strand RNA concentrations confirms that only a small fraction of the viral genomic RNA remains 1 h after infection (Fig. 2C).

Table 2. Numbers of green fluorescent worm cells 7 days after infection at an moi of 0.02 after treatment or mock treatment with anti-glycoprotein antibody at 20 h after infection

Strain	Treatment	
	Mock	Anti-glycoprotein antibody
Wild type	23.7 \pm 2.0	13.5 \pm 1.7
<i>rde-1(ne219)</i>	77.7 \pm 13.4	19.7 \pm 1.4

Values are numbers of cells with distinctly green fluorescence by eye per mm² \pm SEM ($n = 4$ samples). Values are somewhat subjective because the complex shapes of infected cells may have caused some cells to be counted twice.

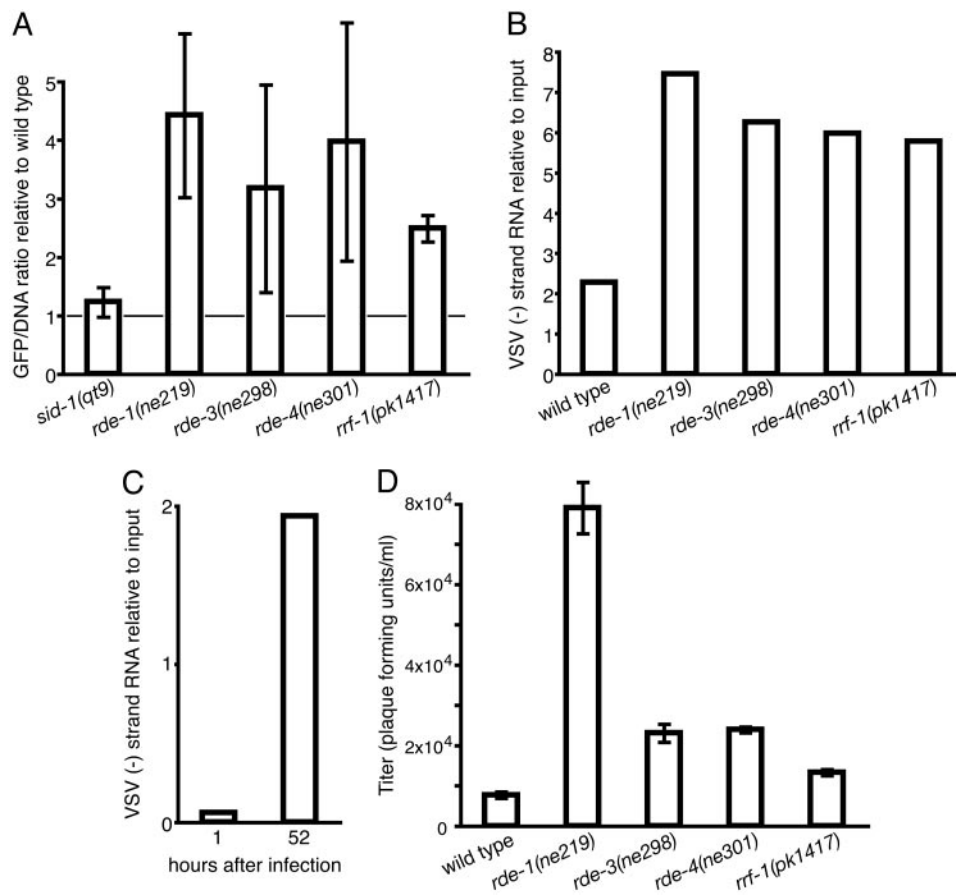


Fig. 2. VSV replication in infected wild-type and RNAi-defective *C. elegans* cells. (A) GFP levels in RNAi-defective mutants relative to wild-type 7 days after infection at moi = 3. Values are ratios of GFP fluorescence to Hoechst 33342 fluorescence, relative to wild type. Error bars represent the 95% confidence interval in *t* distribution based on four to eight worm embryonic cell isolations. Different from wild type in two-tailed *t* tests: *rde-1(ne219)*, $P = 7 \times 10^{-4}$; *rde-3(ne298)*, $P = 0.03$; *rde-4(ne301)*, $P = 0.02$; *rrf-1(pk1417)*, $P = 2 \times 10^{-4}$; *sid-1(qt9)*, $P = 0.07$. Different from *sid-1(qt9)* in two-tailed *t* tests: *rde-1(ne219)*, $P = 9 \times 10^{-4}$; *rde-3(ne298)*, $P = 0.04$; *rde-4(ne301)*, $P = 0.02$; *rrf-1(pk1417)*, $P = 1 \times 10^{-5}$. (B) Quantities of VSV (-) strand RNA in cells 7 days after infection at moi = 3, relative to virus used to infect cells. (C) Quantities of VSV (-) strand RNA in *rde-1(ne219)* cells 1 h and 52 h after infection at moi = 3, relative to virus used to infect cells. (D) Virus titers capable of infecting mammalian cells, in medium 7 days after infection of wild-type and mutant cells at moi = 3. Error bars represent SEM; $n = 4$ cell culture wells. Different from wild type in two-tailed *t* tests: *rde-1(ne219)*, $P = 1 \times 10^{-3}$; *rde-3(ne298)*, $P = 4 \times 10^{-3}$; *rde-4(ne301)*, $P = 7 \times 10^{-6}$; *rrf-1(pk1417)*, $P = 2 \times 10^{-3}$.

Like *rde-1(ne219)* cells, *rde-3(ne298)*, *rde-4(ne301)*, and *rrf-1(pk1417)* cells produce significantly higher titers of virus than do wild-type cells (Fig. 2D), indicating that the VSV replication cycle is disrupted by the activity of several genes needed for RNAi. The strong effect of the *rde-1(ne219)* mutation on virus production is consistent with previous observations that *rde-1(ne219)* has a greater RNAi defect than *rde-3(ne298)* and *rde-4(ne301)* (4).

In addition to testing mutant strains defective for RNAi, we took the complementary approach of adding dsRNA to wild-type cells to silence genes of interest for which mutant alleles either do not exist or are sterile or lethal. First, we used RNAi to confirm that *rde-1* inhibits VSV infection. *rde-1* dsRNA added to wild-type cells results in increased viral GFP expression compared with either wild-type cells treated with irrelevant dsRNA or *sid-1(qt9)* mutant cells treated with *rde-1* dsRNA. Similarly, RNAi of *dcr-1* or RNAi of *C04F12.1* increases viral GFP expression (Fig. 3). *dcr-1* encodes the sole Dicer gene of *C. elegans* (21, 22), whereas *C04F12.1* is an additional Argonaute-like gene recently determined to be required for RNAi (5). Testing *dcr-1* and *C04F12.1* mutants would have been difficult because *dcr-1* mutants are sterile, and *C04F12.1* loss-of-function mutants are not yet available.

Mutants with Enhanced RNAi Show Enhanced Resistance to VSV. If an RNAi-like mechanism protects cells against viral infection, mutants that have an enhanced RNAi response (23–25) would be expected to be more resistant to virus than wild type. To test this, we infected *eri-1(mg366)*, *rrf-3(pk1426)*, and *lin-15B(n744)* mutant cells with VSV. *eri-1* encodes an exonuclease believed to degrade small interfering RNAs in the worm (23). *rrf-3* encodes a predicted RNA-dependent RNA polymerase (24), but the mechanism whereby *rrf-3* inhibits RNAi is unknown. *lin-15B* encodes a part of the retinoblastoma tumor suppressor (Rb) signaling pathway that has recently been found to limit expression of germline components to the germline and probably inhibits somatic RNAi by blocking misexpression of germline RNAi genes in somatic tissues (25). *eri-1(mg366)* and *rrf-3(pk1426)* cells produce slightly less GFP than wild-type cells whereas *lin-15B(n744)* mutant and *lin-15B(n744);eri-1(mg366)* double mutant cells produce dramatically less GFP (Fig. 4). Thus, it appears that greater-than-normal resistance to VSV can be achieved by mutants that have an abnormally sensitive or robust RNAi apparatus.

Conclusions

We conclude that resistance to VSV is correlated with RNAi. Specifically, we show that several genes required for RNAi,

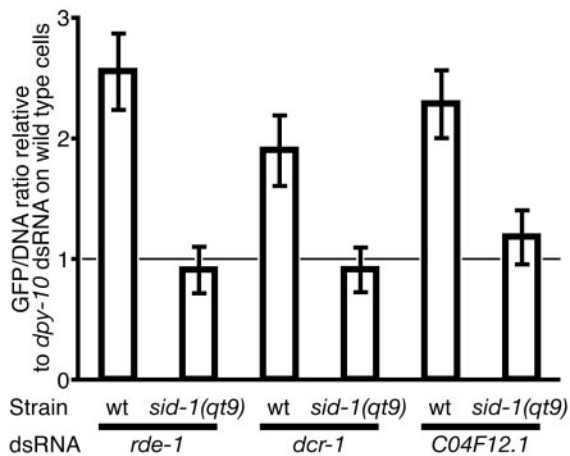


Fig. 3. GFP levels in dsRNA-treated wild-type and *sid-1(qt9)* cell cultures relative to wild type (wt) treated with irrelevant (*dpy-10*) dsRNA 7 days after infection at $\text{moi} = 3$. Values are ratios of GFP fluorescence to Hoechst 33342 fluorescence, relative to wild type. Error bars represent the 95% confidence interval in t distribution based on samples within one experiment, but data are representative of at least two experiments. Different from *dpy-10* dsRNA-treated wild type in two-tailed t tests: *rde-1* dsRNA-treated wild type, $P = 2 \times 10^{-12}$; *dcr-1* dsRNA-treated wild type, $P = 2 \times 10^{-7}$; *C04F12.1* dsRNA-treated wild type, $P = 7 \times 10^{-12}$. Different from corresponding *sid-1(qt9)* cells in two-tailed t tests: *rde-1* dsRNA-treated wild type, $P = 7 \times 10^{-13}$; *dcr-1* dsRNA-treated wild type, $P = 1 \times 10^{-8}$; *C04F12.1* dsRNA-treated wild type, $P = 7 \times 10^{-10}$.

rde-1, *rde-3*, *rde-4*, *rrf-1*, *dcr-1*, and *C04F12.1*, are also required for resistance to a virus. For some of these genes, namely *rde-1*, *rde-4*, *rrf-1*, and *C04F12.1*, no mutant phenotype other than a defect in RNAi was previously known, suggesting that resistance to virus may be a natural and selected function for these RNAi components. These observations imply that the RNAi apparatus may have evolved in part as a nucleic-acid-based innate immune response that confers resistance to some viruses. Although *C. elegans* lacks the adaptive immunity mechanisms that are well known in vertebrates, it is an excellent model animal to study such mechanisms of innate immunity. This experimental system

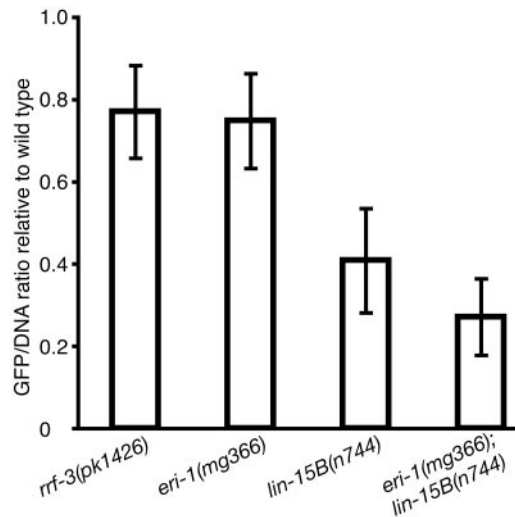


Fig. 4. GFP levels in RNAi enhanced mutants relative to wild type 7 days after infection at $\text{moi} = 6$. Values are ratios of GFP fluorescence to Hoechst 33342 fluorescence, relative to wild type. Error bars represent the 95% confidence interval in t distribution based on samples within one experiment, but data are representative of at least two experiments. Different from wild type in two-tailed t tests: *rrf-3(pk1426)*, $P = 6 \times 10^{-4}$; *eri-1(mg366)*, $P = 3 \times 10^{-4}$; *lin-15B(n744)*, $P = 2 \times 10^{-8}$; *eri-1(mg366); lin-15B(n744)*, $P = 2 \times 10^{-8}$.

for viral infection in *C. elegans* cells opens up the study of viruses to the powerful tools of *C. elegans* genetics and will allow the rapid identification of genes that affect viral infection.

Note Added in Proof. Wilkins *et al.* (26) have recently reported similar findings.

We thank the *Caenorhabditis* Genetics Center for strains, Duo Wang and Gary Ruvkun for strains before publication, Volker Vogt for suggesting the use of VSV, and the National Institutes of Health for funding [Grants R01 GM069891 (to C.P.H.) and AI059371 (to S.P.W.)]. S.P.W. holds an Investigators in the Pathogenesis of Infectious Disease Award from the Burroughs Wellcome Fund.

- Meister, G. & Tuschl, T. (2004) *Nature* **431**, 343–349.
- Mello, C. C. & Conte, D., Jr. (2004) *Nature* **431**, 338–342.
- Rand, T. A., Ginalski, K., Grishin, N. V. & Wang, X. (2004) *Proc. Natl. Acad. Sci. USA* **101**, 14385–14389.
- Tabara, H., Sarkissian, M., Kelly, W. G., Fleenor, J., Grishok, A., Timmons, L., Fire, A. & Mello, C. C. (1999) *Cell* **99**, 123–132.
- Kim, J. K., Gabel, H. W., Kamath, R. S., Tewari, M., Pasquinielli, A., Rual, J. F., Kennedy, S., Dybbs, M., Bertin, N., Kaplan, J. M., *et al.* (2005) *Science* **308**, 1164–1167.
- Jacobs, B. L. & Langland, J. O. (1996) *Virology* **219**, 339–349.
- Lecellier, C. H. & Voinnet, O. (2004) *Immunol. Rev.* **198**, 285–303.
- Fire, A., Xu, S., Montgomery, M. K., Kostas, S. A., Driver, S. E. & Mello, C. C. (1998) *Nature* **391**, 806–811.
- Zamore, P. D. (2001) *Curr. Biol.* **14**, R198–R200.
- Bucher, E., Hemmes, H., de Haan, P., Goldbach, R. & Prins, M. (2004) *J. Gen. Virol.* **85**, 983–991.
- Lu, S. & Cullen, B. R. (2004) *J. Virol.* **78**, 12868–12876.
- Keene, K. M., Foy, B. D., Sanchez-Vargas, I., Beaty, B. J., Blair, C. D. & Olson, K. E. (2004) *Proc. Natl. Acad. Sci. USA* **101**, 17240–17245.
- Christensen, M., Estevez, A., Yin, X., Fox, R., Morrison, R., McDonnell, M., Gleason, C., Miller, D. M., III, & Strange, K. (2002) *Neuron* **33**, 503–514.
- Whelan, S. P., Ball, L. A., Barr, J. N. & Wertz, G. T. (1995) *Proc. Natl. Acad. Sci. USA* **92**, 8388–8392.
- Levy, A. D., Yang, J. & Kramer, J. M. (1993) *Mol. Biol. Cell* **4**, 803–817.
- Sijen, T., Fleenor, J., Simmer, F., Thijssen, K. L., Parrish, S., Timmons, L., Plasterk, R. H. & Fire, A. (2001) *Cell* **107**, 465–476.
- Chen, C. C., Simard, M. J., Tabara, H., Brownell, D. R., McCollough, J. A. & Mello, C. C. (2005) *Curr. Biol.* **15**, 378–383.
- Tabara, H., Yigit, E., Siomi, H. & Mello, C. C. (2002) *Cell* **109**, 861–871.
- Winston, W. M., Molodowitch, C. & Hunter, C. P. (2002) *Science* **295**, 2456–2459.
- Feinberg, E. H. & Hunter, C. P. (2003) *Science* **301**, 1545–1547.
- Ketting, R. F., Fischer, S. E., Bernstein, E., Sijen, T., Hannon, G. J. & Plasterk, R. H. (2001) *Genes Dev.* **15**, 2654–2659.
- Knight, S. W. & Bass, B. L. (2001) *Science* **293**, 2269–2271.
- Kennedy, S., Wang, D. & Ruvkun, G. (2004) *Nature* **427**, 645–649.
- Simmer, F., Tijsterman, M., Parrish, S., Koushika, S. P., Nonet, M. L., Fire, A., Ahringer, J. & Plasterk, R. H. (2002) *Curr. Biol.* **12**, 1317–1319.
- Wang, D., Kennedy, S., Conte, D., Jr., Kim, J. K., Gabel, H. W., Kamath, R. S., Mello, C. C. & Ruvkun, G. (2005) *Nature* **436**, 593–597.
- Wilkins, C., Dishongh, R., Moore, S. C., Whitt, M. A., Chow, M. & Machaca, K. (2005) *Nature* **436**, 1044–1047.